PHYSICAL REVIEW D VOLUME 44, NUMBER 2 15 JULY 1991

Light-front limit in a rest frame

Mikolaj Sawicki*
Department of Physics, Texas A&M University, College Station, Texas 77843-4242
(Received 19 February 1991)

Covariant perturbation theory is formulated using a new set of space-time coordinates. This corresponds to a quantization on any flat spacelike surface in Minkowski space. One limit of the theory reproduces the usual instant (equal-time) dynamics, whereas a different limit gives light-front dynamics. Neither the infinite-momentum frame nor infinite momenta are involved. In particular a smooth parametric transformation from the instant to light-front picture is given for a system at rest.

I. INTRODUCTION

Weinberg [1] considered the two-body scattering amplitude within the scalar ϕ^3 model in the lowest order of old-fashioned perturbation theory [time-ordered perturbation theory (TOPT)]. He investigated a particular limit $P^3 \to \infty$ of individual diagrams constructed according to TOPT rules, and demonstrated that, in such a limit, hereafter referred to as an "infinite-momentum frame," each diagram either approaches a finite value or simply vanishes. Consequently, he formulated the rules for calculating TOPT in the "infinite-momentum frame."

Brodsky, Roskies, and Suaya [2] considered the infinite-momentum limit for spin-$\frac{1}{2}$ theories and for the ϕ^3 vertex as well. In particular they established a connection between Feynman rules and TOPT rules in the infinite-momentum frame, for the case of a triangle diagram describing a QED vertex in the third order of perturbation theory. They have shown that out of 6 TOPT diagrams corresponding to a simple Feynman vertex triangle diagram, only 2 diagrams survive when the limit $P^3 \to \infty$ is taken. They subsequently demonstrated that upon choosing the momentum of the incoming photon to be purely transverse one is able to reduce the Feynman diagram to a single TOPT diagram in the infinite-momentum frame.

Chang and Ma [3] studied the Feynman rules in terms of the new variables $p^0 + p^3$ and $p^0 - p^3$ in the ϕ^3 model and in quantum electrodynamics. In the ϕ^3 model they recovered Weinberg's rules at infinite momentum upon integrating covariant propagators over the $p^0 - p^3$ variable. Likewise Kogut and Soper [4] introduced the light-front variables $x^+ = \frac{1}{\sqrt{2}}(ct + z)$ and $x^- = \frac{1}{\sqrt{2}}(ct - z)$. They considered a Feynman diagram for a two-body radiative process and integrated the propagators over x^-. In this way they established the rules for perturbative calculations on the light front, which turned out to be fully equivalent to the "infinite-momentum-frame" rules. They also deduced what the field commutators should be at equal x^+ in order to get a consistent formalism. Chang, Root, and Yan [5] subsequently employed the Schwinger action principle to actually derive the commutation rules postulated by Kogut and Soper.

In this way the instant and light-front-quantization methods have been demonstrated to be fully equivalent, with the link between both formulations being provided by the infinite-momentum frame. Therefore the limit $P^3 \to \infty$ has been considered a necessary evil, although in fact no invariant quantity is getting large, as pointed out in Ref. [2]. Nevertheless a description in terms of light-front variables has been frequently associated with the infinite-momentum limit, thus obscuring an underlying physical picture and causing some confusion about actual motion of objects involved.

It is the purpose of the present paper to demonstrate that the transition from the equal-time perturbation theory to the light-front perturbation theory could be achived without any reference to the infinite-momentum-frame limit whatsover. Not only all involved momenta will remain finite, but the system under consideration will be in fact at rest.

As the case in study I will consider the triangle diagram for the ϕ^3 model. In Sec. II, I will construct a covariant expression for the scattering amplitude. I will then project this amplitude onto the light front and demonstrate how such a projection results in 2 light-front diagrams. In Sec. III, I will alternatively project the covariant amplitude onto the equal-time surface and demonstrate how this projection results in 6 TOPT diagrams discussed in Ref. [2]. Then in Sec. IV, I will introduce a one-parameter family of coordinates and generalize the projections described above. I will analyze a structure of resulting diagrams and I will show how to transform a TOPT picture into a light-front picture upon merely changing a value of the parameter α, but keeping the system at rest.

II. COVARIANT AMPLITUDE AND LIGHT-FRONT PROJECTION

Consider the contribution of the Feynman diagram of Fig. 1 in the scalar ϕ^3 coupling to the bound-state current of the scalar bound state of the mass M:

$$J^\mu(0) = \int d^4k \frac{1}{(k+q)^2 - m^2 + i\epsilon} (2k^\mu + q^\mu) \frac{1}{k^2 - m^2 + i\epsilon} \frac{1}{(P-k)^2 - m^2 + i\epsilon}. \quad (1)$$

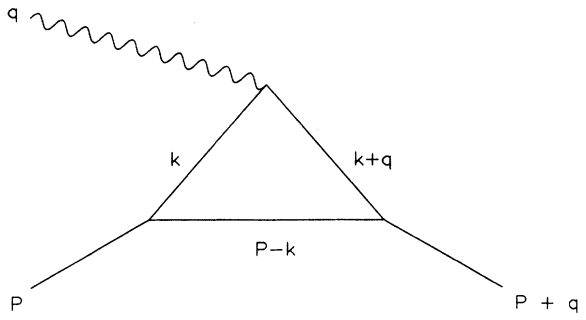

FIG. 1. Feynman triangle diagram for a calculation of a bound-state current.

Let us observe that analogous expression could be derived for the electromagnetic current of the two-body bound state in an exactly solvable model of a relativistic dynamics [6]. An observable, the elastic form factor of the bound state then could be extracted:

$$J^\mu(0) = (2P^\mu + q^\mu)\, F(Q^2), \tag{2}$$

where q^μ is the four-momentum transfer, $Q^2 = -q^2 \geq 0$, P^μ and $P^\mu + q^\mu$ are the initial and final momentum of the bound state, respectively, and $P^2 = (P+q)^2 = M^2$. I introduce now the light-front momenta

$$k^+ = \frac{1}{\sqrt{2}}(k^0 + k^3), \tag{3}$$

$$k^- = \frac{1}{\sqrt{2}}(k^0 - k^3), \tag{4}$$

$$\mathbf{k}_\perp = (k^1, k^2), \tag{5}$$

and I have

$$k^2 = 2k^-k^+ - (\mathbf{k}_\perp)^2, \tag{6}$$

$$d^4k = dk^- dk^+ d^2k_\perp. \tag{7}$$

I integrate Eq. (1) over k^- by residues. The poles are located at

$$k_a^- = -q^- + \frac{m^2 + (\mathbf{k}_\perp + \mathbf{q}_\perp)^2}{2(k^+ + q^+)} - \frac{i\epsilon}{2(k^+ + q^+)}, \tag{8}$$

$$k_b^- = \frac{m^2 + (\mathbf{k}_\perp)^2}{2k^+} - \frac{i\epsilon}{2k^+}, \tag{9}$$

$$k_c^- = P^- - \frac{m^2 + (\mathbf{P}_\perp - \mathbf{k}_\perp)^2}{2(P^+ - k^+)} + \frac{i\epsilon}{2(P^+ - k^+)}. \tag{10}$$

Each of the poles may be located either in the lower or upper half of the complex k^- plane, depending on values of k^+, q^+, and P^+. To be more specific I observe that P^+ is always positive, $P^+ \geq M$. Without any loss of generality I will assume $q^+ \geq 0$. Then the poles are located as illustrated in Fig. 2. Configurations (i) and (iv) give no contribution to the k^- integral, as I could always close the contour from above for (i) and from below for (iv), avoiding any pole. Thus only configurations (ii) and (iii) contribute. I close the contour from below for configuration (ii), picking the residue at k_a^-, and from above for configuration (iii), picking the residue at k_c^-. This is how 2 light-front diagrams appear. Moreover, configuration (ii) never appears if $q^+ = 0$. Equivalently, the contribution from the pole at k_a^- vanishes for $q^+ \to 0$, and only a single diagram remains. The result for the $\mu = +, x, y$ component of the current (1) reads

$$J^\mu(0) = 2\pi i\, (I_{ii} + I_{iii})^\mu, \tag{11}$$

where I_{ii}^μ is the contribution from the configuration of Fig. 2-(ii):

$$I_{ii}^\mu = -\int_0^{P^+} dk^+\, d^2k_\perp \frac{2k^\mu + q^\mu}{2k^+\, 2(k^+ + q^+)\, 2(P^+ - k^+)} \frac{1}{(P^- + q^-) - \left(q^- + \dfrac{m^2 + (\mathbf{P}_\perp - \mathbf{k}_\perp)^2}{2(P^+ - k^+)} + \dfrac{m^2 + k_\perp^2}{2k^+}\right)}$$

$$\times \frac{1}{(P^- + q^-) - \left(\dfrac{m^2 + (\mathbf{P}_\perp - \mathbf{k}_\perp)^2}{2(P^+ - k^+)} + \dfrac{m^2 + (\mathbf{k}_\perp + \mathbf{q}_\perp)^2}{2(k^+ + q^+)}\right)}, \tag{12}$$

and I_{iii} is the contribution from the configuration of Fig.2-(iii):

$$I_{iii}^\mu = -\int_0^{q^+} dk^+\, d^2k_\perp \frac{q^\mu - 2k^\mu}{2k^+\, 2(q^+ - k^+)\, 2(P^+ + k^+)} \frac{1}{(P^- + q^-) - \left(P^- + \dfrac{m^2 + (\mathbf{q}_\perp - \mathbf{k}_\perp)^2}{2(q^+ - k^+)} + \dfrac{m^2 + k_\perp^2}{2k^+}\right)}$$

$$\times \frac{1}{(P^- + q^-) - \left(\dfrac{m^2 + (\mathbf{P}_\perp + \mathbf{k}_\perp)^2}{2(P^+ + k^+)} + \dfrac{m^2 + (\mathbf{q}_\perp - \mathbf{k}_\perp)^2}{2(q^+ - k^+)}\right)}. \tag{13}$$

One easily recognizes expressions (12) and (13) as the contributions from the light-front (or infinite-momentum-frame) diagrams (a) and (b) of Fig. 3, respectively. I conclude this section noting that the alternate choice of parametrization with $q^+ \leq 0$ yields a fully equivalent result. Finally, assuming that the target is initially at rest I have $P^3 = 0$, $\mathbf{P}_\perp = 0$, and $P^0 = M$, and the variables P^+, P^- in Eqs. (12) and (13) take the value

$$P^+ = P^- = M/\sqrt{2} \text{ (target rest frame).} \tag{14}$$

III. EQUAL-TIME PROJECTION

Here I derive equivalent equal-time picture of the process discussed above. Again, I consider Eq. (1) but now integrate over the variable k^0. Each Feynman propagator gives rise to 2 poles in the complex k^0 plane, so I have three pairs of poles:

$$k_1^0 = -q^0 + \omega(\mathbf{k}+\mathbf{q}) - i\epsilon, \tag{15}$$
$$k_2^0 = -q^0 - \omega(\mathbf{k}+\mathbf{q}) + i\epsilon, \tag{16}$$
$$k_3^0 = \omega(\mathbf{k}) - i\epsilon, \tag{17}$$
$$k_4^0 = -\omega(\mathbf{k}) + i\epsilon, \tag{18}$$
$$k_5^0 = P^0 + \omega(\mathbf{P}-\mathbf{k}) - i\epsilon, \tag{19}$$
$$k_6^0 = P^0 - \omega(\mathbf{P}-\mathbf{k}) + i\epsilon, \tag{20}$$

where $\omega(\mathbf{p}) = (\mathbf{p}^2 + m^2)^{1/2}$. The poles at k_1^0, k_3^0, k_5^0 are always in the lower half plane, and the poles at k_2^0, k_4^0, k_6^0 are always in the upper half plane. Integrating over k^0 by residues and closing the contour from above I have, for the $\mu = 1, 2, 3$ component of the current,

$$J^\mu(0) = 2\pi i\,(I_2 + I_4 + I_6)^\mu, \tag{21}$$

where the integral I_n is given by the residue of the pole at k_n^0. In particular, for the pole at k_6^0 I have

$$I_6^\mu = \int d^3k \frac{2k^\mu + q^\mu}{(k_6^0 - k_1^0)\,(k_6^0 - k_2^0)\,(k_6^0 - k_3^0)\,(k_6^0 - k_4^0)\,(k_6^0 - k_5^0)}, \tag{22}$$

and likewise for I_2^μ and I_4^μ. Using Eqs. (15)–(20) I obtain

$$I_6^\mu = -\int d^3k\,(2k^\mu + q^\mu) \frac{1}{2\omega(\mathbf{P}-\mathbf{k})\,[2\omega(\mathbf{k}) + D_3]\,[2\omega(\mathbf{k}+\mathbf{q}) + D_2]\,D_3\,D_2}, \tag{23}$$

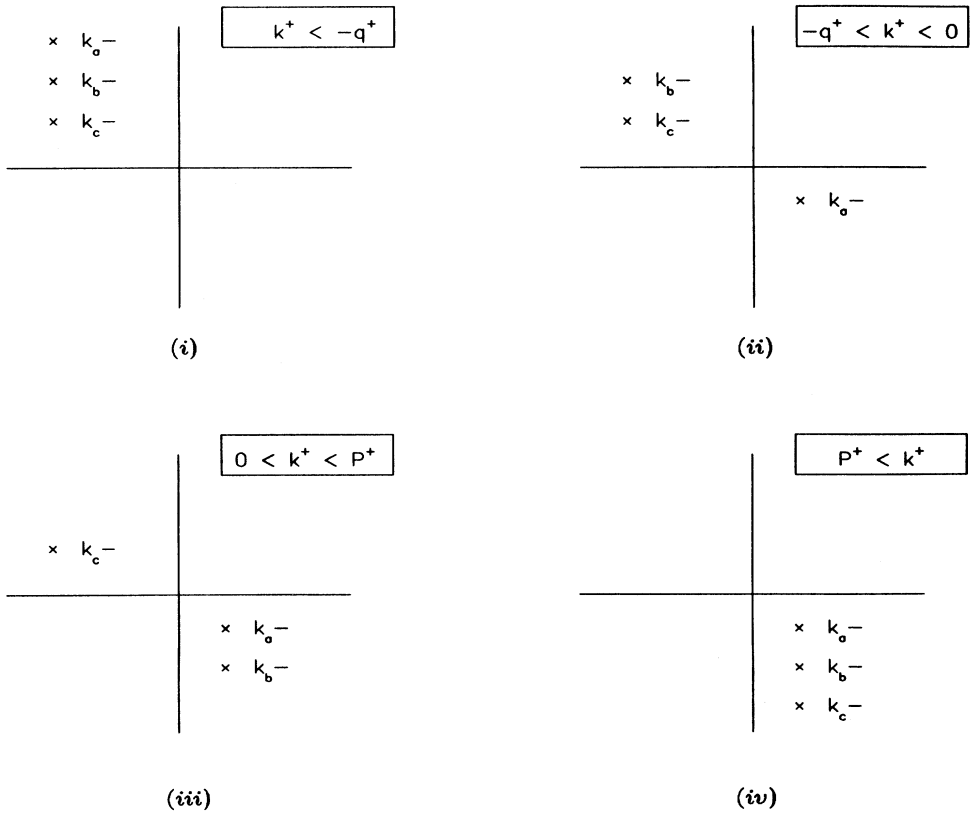

FIG. 2. Locations of the poles in the complex k^- plane.

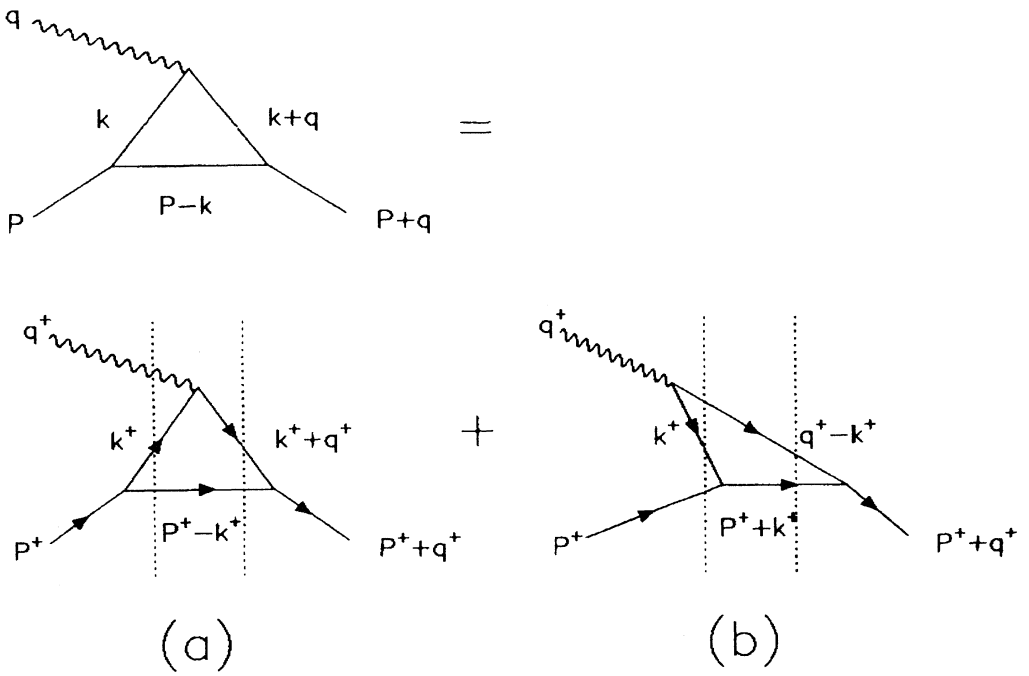

FIG. 3. Light-front diagrams equivalent to the Feynman triangle diagram of Fig. 1.

where D_2 and D_3 are the TOPT energy denominators of two- and three-body propagators, respectively

$$D_2 = (q^0 + P^0) - [\omega(\mathbf{P}-\mathbf{k}) + \omega(\mathbf{k}+\mathbf{q})], \tag{24}$$

$$D_3 = (q^0 + P^0) - [q^0 + \omega(\mathbf{k}) + \omega(\mathbf{P}-\mathbf{k})]. \tag{25}$$

The structure of Eq. (23) is very similar to the corresponding TOPT diagram (f) of Fig. 4,

$$I_6^{\mu,\,\mathrm{TOPT}} = -\int d^3k\,(2k^\mu + q^\mu)\frac{1}{2\omega(\mathbf{k}+\mathbf{q})\,2\omega(\mathbf{k})\,2\omega(\mathbf{P}-\mathbf{k})\,D_2\,D_3}. \tag{26}$$

The only difference is in propagators of two internal lines with momenta $\mathbf{k}$ and $\mathbf{k}-\mathbf{q}$. These are the internal lines in the triangle cut only once by the intermediate states, indicated by the dotted lines in the Fig. 4, and the propagator of such an internal line is shifted from its TOPT value precisely by the value of multiparticle intermediate propagator that cuts the line.

Likewise, the remaining two integrals I_2 and I_4 correspond to the TOPT diagrams (b) and (d) of Fig. 4, respectively. Again, the propagators of the internal lines which are cut only once are shifted from the TOPT values in the manner described above.

The fact that the 3 integrals I_2, I_4, and I_6 have partially distorted single-particle propagators is a welcome one. After all, one expects that Eq. (21) corresponds to all 6 proper TOPT diagrams of Fig. 4. Indeed, after painful algebra (I did it running MACSYMA—the symbolic manipulation package on Vax) one arrives at the expected result:

$$J^\mu(0) = 2\pi i \sum_{n=1}^{6} I_n^{\mu,\,\mathrm{TOPT}}, \tag{27}$$

where all six TOPT integrals have the proper structure, as exemplified by Eq. (26), and correspond one by one to all 6 diagrams (a)–(f) of Fig. 4.

I have thus demonstrated that the covariant expression Eq. (1) could be cast either into the light-front form, Eq. (11), or into the traditional instant form, Eq.(27). In the next section I will describe how to interpolate between these two extreme cases.

IV. INTERPOLATING VARIABLES AND PROJECTION

Let us consider the parametrization of the momenta

$$k^\eta = \frac{1}{\sqrt{\cosh(2\alpha)}}[k^0 \sinh(\alpha) + k^3 \cosh(\alpha)], \tag{28}$$

$$k^\lambda = \frac{1}{\sqrt{\cosh(2\alpha)}}[k^0 \cosh(\alpha) - k^3 \sinh(\alpha)]. \tag{29}$$

This is a slight modification of the space-time variables recently suggested by Ahluwalia and Ernst [7] in their study of Dirac equation. Thus defined momenta interpolate smoothly between instant and light-front variables:

$$k^\eta \longrightarrow \begin{cases} k^3 & \text{if } \alpha \to 0, \\ k^+ & \text{if } \alpha \to \infty, \end{cases}$$

$$k^\lambda \longrightarrow \begin{cases} k^0 & \text{if } \alpha \to 0, \\ k^- & \text{if } \alpha \to \infty. \end{cases}$$

Further I have

$$k^2 = \frac{(k^\lambda)^2 - (k^\eta)^2}{\cosh(2\alpha)} + 2k^\lambda k^\eta \tanh(2\alpha) - \mathbf{k}_\perp^2 \tag{30}$$

$$\longrightarrow \begin{cases} (k^0)^2 - (k^3)^2 - \mathbf{k}_\perp^2 & \text{if } \alpha \to 0, \\ 2k^- k^+ - \mathbf{k}_\perp^2 & \text{if } \alpha \to \infty, \end{cases} \tag{31}$$

$$dk^0\, dk^3 = dk^\eta dk^\lambda \tag{32}$$

$$\longrightarrow \begin{cases} dk^0\, dk^3 & \text{if } \alpha \to 0, \\ dk^- dk^+ & \text{if } \alpha \to \infty. \end{cases} \tag{33}$$

I change the variables in the Feynman propagators in Eq. (1) and integrate over k^λ. Using Eq. (30) I rewrite the second denominator in Eq. (1) as

$$k^2 - m^2 + i\epsilon = \frac{1}{\cosh(2\alpha)} (k^\lambda - k_3^\lambda)\,(k^\lambda - k_4^\lambda), \tag{34}$$

where the poles for k^λ are located at

$$k_3^\lambda = -k^\eta \sinh(2\alpha) + \cosh(2\alpha) \left((k^\eta)^2 + \frac{m^2 + \mathbf{k}_\perp^2 - i\epsilon}{\cosh(2\alpha)} \right)^{1/2}, \tag{35}$$

$$k_4^\lambda = -k^\eta \sinh(2\alpha) - \cosh(2\alpha) \left((k^\eta)^2 + \frac{m^2 + \mathbf{k}_\perp^2 - i\epsilon}{\cosh(2\alpha)} \right)^{1/2}. \tag{36}$$

The pole at k_3^λ is always located in the lower half plane, whereas the pole at k_4^λ in the upper half plane. Evidently, in the limit of $\alpha \to 0$ the poles k_3^λ, k_4^λ coincide with the poles k_3^0, k_4^0, respectively. In the limit of $\alpha \to \infty$ I have

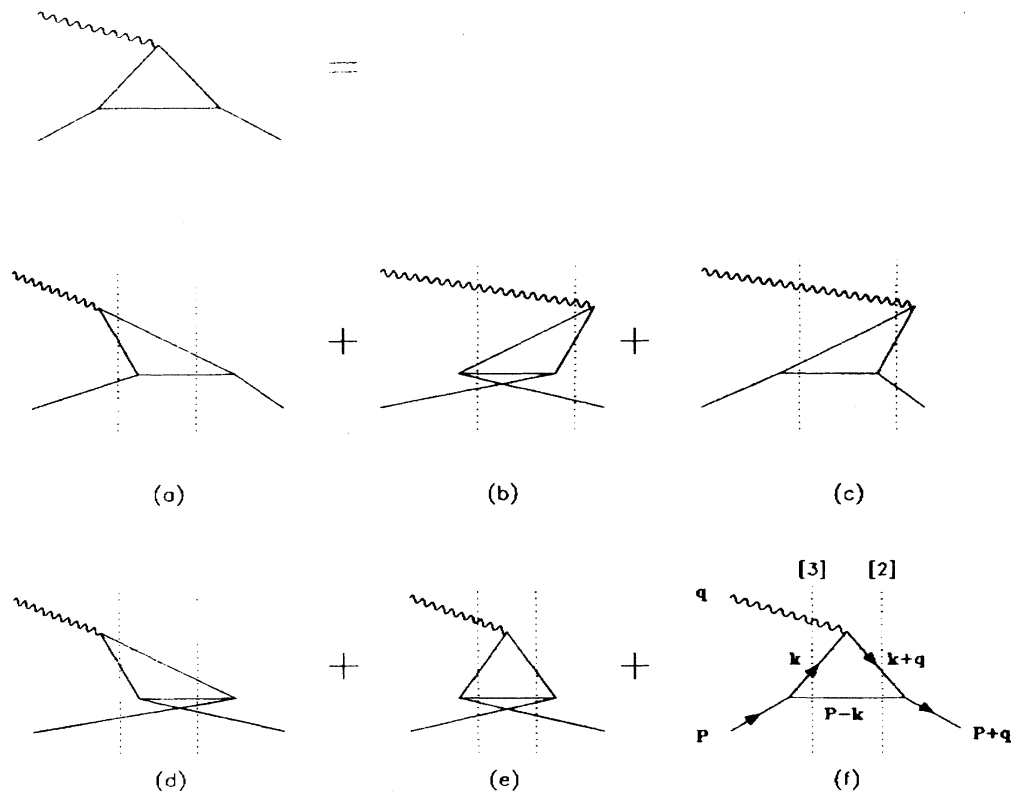

FIG. 4. Time-ordered diagrams equivalent to the Feynman diagram of Fig. 1, cf. Eq. (27). Diagram (f) represents the TOPT contribution given by Eq. (26). The dotted lines indicate intermediate multiparticle propagators. Diagrams (a)–(f) may be associated with contributions from poles at $k_1^0 - k_6^0$, respectively, if single-particle lines are modified as discussed in text.

$$\lim_{\alpha\to\infty} k_3^\lambda = \begin{cases} \dfrac{m^2+\mathbf{k}_\perp^2-i\epsilon}{2|k^\eta|} & \text{if } k^\eta > 0, \\ |k^\eta|\exp(2\alpha) + \dfrac{m^2+\mathbf{k}_\perp^2-i\epsilon}{2|k^\eta|} & \text{if } k^\eta < 0 \text{ (runaway pole)}, \end{cases} \tag{37}$$

and likewise for the other pole

$$\lim_{\alpha\to\infty} k_4^\lambda = \begin{cases} |k^\eta|\exp(2\alpha) - \dfrac{m^2+\mathbf{k}_\perp^2-i\epsilon}{2|k^\eta|} & \text{if } k^\eta > 0 \text{ (runaway pole)}, \\ -\dfrac{m^2+\mathbf{k}_\perp^2-i\epsilon}{2|k^\eta|} & \text{if } k^\eta < 0. \end{cases} \tag{38}$$

Thus for any value of k^η one pole in the pair migrates to $\pm\infty$ for $\alpha\to\infty$. Likewise, the denominator of the first Feynman propagator in Eq. (1) takes the form

$$(k+q)^2 - m^2 + i\epsilon = \frac{1}{\cosh(2\alpha)}\,(k^\lambda - k_1^\lambda)\,(k^\lambda - k_2^\lambda), \tag{39}$$

and the poles for k^λ are located at

$$k_{1,2}^\lambda = -q^\lambda - (k^\eta+q^\eta)\sinh(2\alpha) \pm \cosh(2\alpha)\left((k^\eta+q^\eta)^2 + \frac{m^2+(\mathbf{k}_\perp+\mathbf{q}_\perp)^2-i\epsilon}{\cosh(2\alpha)}\right)^{1/2}. \tag{40}$$

Again, for $\alpha\to 0$ the poles k_1^λ, k_2^λ coincide with the poles k_1^0, k_2^0, respectively. In the limit of $\alpha\to\infty$ I have

$$\lim_{\alpha\to\infty} k_1^\lambda = \begin{cases} -q^\lambda + \dfrac{m^2+(\mathbf{k}_\perp+\mathbf{q}_\perp)^2-i\epsilon}{2|k^\eta+q^\eta|} & \text{if } k^\eta+q^\eta > 0, \\ |k^\eta+q^\eta|\exp(2\alpha) - q^\lambda + \dfrac{m^2+(\mathbf{k}_\perp+\mathbf{q}_\perp)^2-i\epsilon}{2|k^\eta+q^\eta|} & \text{if } k^\eta+q^\eta < 0 \text{ (runaway pole)} \end{cases} \tag{41}$$

and likewise for the other pole

$$\lim_{\alpha\to\infty} k_2^\lambda = \begin{cases} -|k^\eta+q^\eta|\exp(2\alpha) - q^\lambda - \dfrac{m^2+(\mathbf{k}_\perp+\mathbf{q}_\perp)^2-i\epsilon}{2|k^\eta+q^\eta|} & \text{if } k^\eta+q^\eta > 0 \text{ (runaway pole)}, \\ -q^\lambda - \dfrac{m^2+(\mathbf{k}_\perp+\mathbf{q}_\perp)^2-i\epsilon}{2|k^\eta+q^\eta|} & \text{if } k^\eta+q^\eta < 0. \end{cases} \tag{42}$$

Finally, the denominator of the third propagator takes the form

$$(P-k)^2 - m^2 + i\epsilon = \frac{1}{\cosh(2\alpha)}\,(k^\lambda - k_5^\lambda)\,(k^\lambda - k_6^\lambda), \tag{43}$$

and the poles for k^λ are located at

$$k_{5,6}^\lambda = P^\lambda + (P^\eta - k^\eta)\sinh(2\alpha) \pm \cosh(2\alpha)\left((P^\eta-k^\eta)^2 + \frac{m^2+(\mathbf{P}_\perp-\mathbf{k}_\perp)^2-i\epsilon}{\cosh(2\alpha)}\right)^{1/2}. \tag{44}$$

Again, for $\alpha\to 0$ the poles k_5^λ, k_6^λ coincide with the poles k_5^0, k_6^0, respectively. In the limit of $\alpha\to\infty$ I have

$$\lim_{\alpha\to\infty} k_5^\lambda = \begin{cases} P^\lambda + \dfrac{m^2+(\mathbf{P}_\perp-\mathbf{k}_\perp)^2-i\epsilon}{2|P^\eta-k^\eta|} & \text{if } k^\eta > P^\eta, \\ |P^\eta-k^\eta|\exp(2\alpha) + P^\lambda + \dfrac{m^2+(\mathbf{P}_\perp-\mathbf{k}_\perp)^2-i\epsilon}{2|P^\eta-k^\eta|} & \text{if } k^\eta < P^\eta \text{ (runaway pole)} \end{cases} \tag{45}$$

and likewise for the other pole

$$\lim_{\alpha\to\infty} k_6^\lambda = \begin{cases} -|P^\eta - k^\eta|\exp(2\alpha) + P^\lambda - \dfrac{m^2(\mathbf{P}_\perp - \mathbf{k}_\perp)^2 - i\epsilon}{2|P^\eta - k^\eta|} & \text{if } k^\eta > P^\eta \text{ (runaway pole),} \\ P^\lambda - \dfrac{m^2 + (\mathbf{P}_\perp - \mathbf{k}_\perp)^2 - i\epsilon}{2|P^\eta - k^\eta|} & \text{if } k^\eta < P^\eta. \end{cases} \tag{46}$$

In any case, the poles at k_1^λ, k_3^λ, and k_5^λ are always located in the lower half plane, whereas the poles at k_2^λ, k_4^λ, and k_6^λ are always in the upper half plane. I have therefore

$$J^\mu(0) = 2\pi i\,[\mathrm{Res}(k_2^\lambda) + \mathrm{Res}(k_4^\lambda) + \mathrm{Res}(k_6^\lambda)]^\mu = -2\pi i\,[\mathrm{Res}(k_1^\lambda) + \mathrm{Res}(k_3^\lambda) + \mathrm{Res}(k_5^\lambda)]^\mu. \tag{47}$$

Integrating over k^λ for $\alpha = 0$ I recover the pole structure and the results of the TOPT described in Sec. III. One could also perform the k^λ integration for any finite value of α. That would express the covariant amplitude in terms of 6 diagrams corresponding to a "x_λ-ordered perturbation theory," with vertices ordered according to values of the space-time variable x_λ conjugated to the momentum space variable k^λ, where

$$x_\lambda = \frac{x^0\cosh(\alpha) + x^3\sinh(\alpha)}{\sqrt{\cosh(2\alpha)}}. \tag{48}$$

I now turn to investigate the light-front limit of $\alpha \to \infty$. For illustration consider the pole at k_6^λ. Using Eq. (34), (39), and (43) I write the residue in the form

$$\mathrm{Res}(k_6^\lambda) = \int dk^\eta \int d^2k_\perp (2k^\mu + q^\mu) \frac{\cosh(2\alpha)^3}{(k_6^\lambda - k_1^\lambda)(k_6^\lambda - k_2^\lambda)(k_6^\lambda - k_3^\lambda)(k_6^\lambda - k_4^\lambda)(k_6^\lambda - k_5^\lambda)}. \tag{49}$$

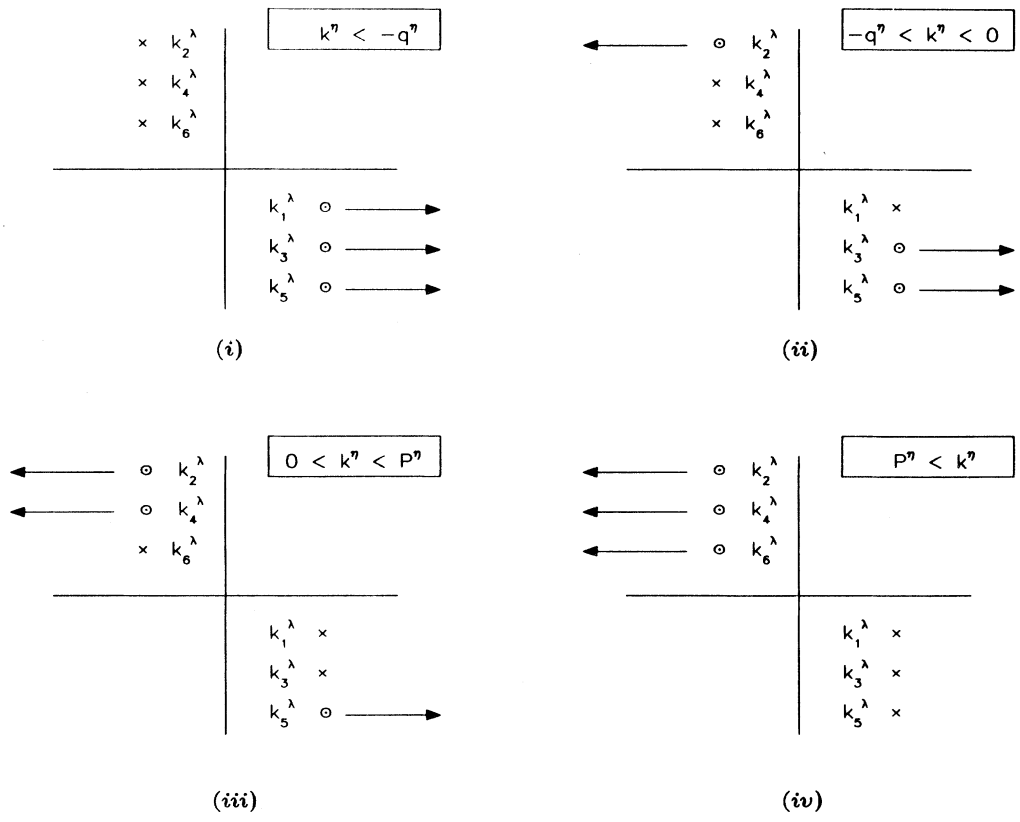

FIG. 5. Locations of the poles in the complex k^λ plane. Arrows indicate runaway poles.

Out of 6 pole locations k_i^λ entering the denominator of Eq. (49), 3 are always runaway locations. Which 3 are runaway is determined by the values of k^η, q^η, and P^η. Clearly, P^η is always positive, and again I am free to assume that $q^\eta \geq 0$. I have then 4 possible distributions of runaway poles, depicted in Fig. 5. To account for that I have to split the integration over k^η in Eq. (49) into 4 parts:

$$\int dk^\eta = \int_{-\infty}^{-q^\eta} dk^\eta + \int_{-q^\eta}^{0} dk^\eta + \int_{0}^{P^\eta} dk^\eta + \int_{P^\eta}^{+\infty} dk^\eta, \tag{50}$$

with definite integrals corresponding to 4 arrangements (*i*)–(*iv*) of Fig. 5, respectively.

Consider arrangement (*iii*). The pole at k_6^λ is then a fixed pole and each of 3 runaway poles now located at $k_2^\lambda, k_4^\lambda, k_5^\lambda$ enters the denominator of Eq. (49) only once, each contributing the factor proportional to $\exp(2\alpha)$, cf. Eqs. (34), (39), and (43). These 3 exponential factors cancel the $\cosh(2\alpha)^3$ term in numerator and I am left with a finite contribution which we recognize as product of 3 internal lines propagators in the light-front limit. The remaining two terms in the denominator, $(k_6^\lambda - k_1^\lambda)\,(k_6^\lambda - k_3^\lambda)$ are finite and correspond to multiparticle propagator of an intermediate state. In this way I arrive at the finite contribution given by Eq. (12) of Sec. II, corresponding to the light-front diagram (a) of Fig. 3.

On the other hand, for arrangement (*iv*) the pole at k_6^λ is a runaway pole itself, thus contributing the factor $\exp(2\alpha)$ to all 5 products in the denominator of Eq. (49). The integrand vanishes as $\exp(-4\alpha)$ and gives no contribution in the limit of $\alpha \to \infty$.

I conclude that residues at runaway poles give no contribution to the integral over k^λ:

$$\lim_{\alpha\to\infty} \mathrm{Res}(k^\lambda_{\mathrm{runaway}}) = 0. \tag{51}$$

On the other hand, while calculating a residue at a fixed pole, runaway terms nicely cooperate to yield single-particle light-front propagators. It follows immediately that configurations (*i*) and (*iv*) give no contribution to Eq. (47). Closing the contour from above for Fig. 5-(*iii*) I pick the pole at k_6^λ as discussed above. For configuration (*ii*) I close contour from below, pick the pole at k_1^λ and arrive at Eq. (13), which represents the second light-front diagram (b) of Fig. 3.

V. CONCLUSION

Introducing a family of variables defined as linear combinations of components of four-momentum and characterized by the parameter α, I considered a perturbation theory for any value of the parameter α, corresponding to a quantization on a flat-spacelike surface in Minkowski space. I demonstrated how instant dynamics and light-front dynamics are recovered upon considering the limits $\alpha \to 0$ and $\alpha \to \infty$, respectively. An illustration has been given for a system at rest, and neither infinite-momentum frame nor infinite momenta were involved. Thus the transition to the light-front description of relativistic dynamics could be thought of as merely smooth change of coordinates.

* Electronic address: sawicki@tamphys.bitnet.

[1] S. Weinberg, Phys. Rev. **150**, 1313 (1966).
[2] S. J. Brodsky, R. Roskies, and R. Suaya, Phys. Rev. D **8**, 4574 (1973).
[3] S. J. Chang and S. K. Ma, Phys. Rev. **180**, 1506 (1969).
[4] J. B. Kogut and D. E. Soper, Phys. Rev. D **1**, 2901 (1970).
[5] S. J. Chang, R. G. Root, and T. M. Yan, Phys. Rev. D **7**, 1133 (1973).
[6] S. Glazek and M. Sawicki, Phys. Rev. D **41**, 2563 (1990).
[7] D. V. Ahluwalia and D. J. Ernst, Report No. CTP-TAMU 91/90 (unpublished).